Asian Journal of Chemistry; Vol. 33, No. 11 (2021), 2746-2754

ASIAN JOURNAL OF CHEMISTRY

https://doi.org/10.14233/ajchem.2021.23387

Metal Complexes of Schiff Bases of 3-Hydroxyquinoxaline-2-carboxaldehyde Encapsulated in Zeolite Y Cages: Potential Catalyst for Removing Phenol from Effluent Media

N.R. SUJA*, T.K. BINDU SHARMILA and S.R. AMRUTHA

Post Graduate and Research Department of Chemistry, Maharaja's College, Ernakulam,Kochi-682011, India

*Corresponding author: E-mail: drsuja@maharajas.ac.in

Received: 27 June 2021; *Accepted*: 18 August 2021; *Published online*: 20 October 2021; AJC-20558

Transition metal complexes are known to be efficient catalyst for many organic transformations. Encapsulation of metal complexes in zeolite cage brings many significant modifications in the structure of the metal complexes, which are very interesting from the catalytic point of view. This study aims in a comparative evaluation of the influence of structure of neat and encapsulated complexes in their catalytic activity. Phenol is one of the major industrial pollutants. Heterogenizing transition metal Schiff bases by encapsulation inside the zeolite would help to minimize the reuse problem of transition metal complexes. This article deals with the synthesis, characterization and catalytic activity studies of Co(II), Ni(II) and Cu(II) complexes of 3-hydroxyquinoxaline-2-carboxaldehyde with ethylenediamine (L1) and an *o*-phenylene diamine (L2).

Keywords: 3-Hydroxyquinoxaline-2-carboxaldehyde, Schiff bases, Zeolite encapsulation, Catalysis, Phenol hydroxylation.

INTRODUCTION

Catalysis is an area of research continues to be a premier frontier area of chemistry, which has revolutionized the modern chemical industries. Transition metal complexes play a major role as catalyst. Studies proves that the disadvantage with such homogeneous catalyst is that they cannot be reused and heterogenizing these catalyst with the help of supports can be used to overcome this disadvantage [1-3]. The potential for coupling the shape selectivity associated with well-defined cages and channels of zeolite with the reactivity of metal complex makes these molecular sieves particularly attractive as active solid supports [4-6]. The distinct advantage of zeolite over conventional support materials is that a metal complex can be physically trapped in the pores and not necessarily bound to the oxide surface [7,8]. Another advantage of zeolites is the high thermal stability, well defined and large internal surface area and potential to impose size and shape selectivity on the product distribution due to the molecular sieving effect [9-12]. Such catalysts have been used in many applications like gas sensors [13], in environmental pollution controls [14], as mimics of biological enzymes [15,16] and as catalyst in many organic reactions [17,18] like oxidation, alkylation, hydroxylation and hydrogenation.

In metal complexes with tetradentate Schiff bases like salen, the ligands are in their ionized form with the four donor atoms, which are nearly coplanar [19-21]. The relative flexibility of such ligands allows distortion in the structure of complexes [22,23]. The extent of distortion depends on the nature of metal and the bulkiness of the apical and axial ligands and also on the interaction of the ethylene bridge substituent with apical ligands. Such distortions play a significant role in reversible oxygenation exhibited by Schiff base complexes [24-26].

Schiff bases derived from 3-hydroxyquinoxaline-2-carboxaldehyde which is structurally similar to salicylaldehyde are expected to be weaker than those derived from salicylaldehyde [27]. As a result there exists the possibility for spin cross over. Studies conducted on the metal complexes of the above ligand have been reported earlier to show this interesting property. Further, many of them were reported to be dimeric complexes. It was, therefore, considered worthwhile to encapsulate the metal complexes of Schiff bases derived from 3-hydroxyquinoxaline-2-carboxaldehyde inside zeolite Y cages and study whether there is any structural change imposed due to the confinement inside the zeolite framework and also to assess the influence of encapsulation on their spin properties. The present article describes the heterogenization of Co(II), Cu(II)

and Ni(II) complexes of Schiff bases of 3-hydroxyquinoxaline-2-carboxaldehyde with *o*-phenylenediamine and ethylenediamine by encapsulating them inside the cages of zeolite-Y.

EXPERIMENTAL

All the chemicals and solvents used were of analytical grade. All the metal chlorides used were purchased from E-Merck. Zeolite-Y was purchased from Sud Chemie India (Pvt.) Ltd., India, sodium pyruvate (SRL), *o*-phenylenediamine (Lobachemie), bromine solution (Merck), glacial acetic acid (99% Merck), $CaCO_3$ precipitated (E-Merck) were used. The aldehyde 3-hydroxyquinoxaline-2-carboxaldehyde was synthesized according to a reported procedure [28], the amines used for the synthesis of the Schiff bases were ethylenediamine (BDH) and *o*-phenylenediamine (Loba Chemie). For catalytic activity studies phenol (E-Merck) and 30% aqueous H_2O_2 (E-Merck) was used. Elemental analysis was performed using ICP-AES and CHN analysis (Central Drug Research Institute, Lucknow). Surface area measurements were done using Micromeritics Gemini 2360 and IR studies using Shimadzu 8000 FTIR. Electronic spectra were recorded using a Carry Win Spectrometer in diffuse reflectance mode and EPR at liquid N_2 temperature using a Varian-109X/Q band at RSIC, IIT Chennai, X-ray analysis Rigada D Max C and TG using Shimadzu TGA-50 at a heating rate of 20 ºC in an inert atmosphere using Pt crucible.

Preparation of metal exchanged zeolite Y: The synthetic Y type zeolite was stirred in 0.1 mol dm^{-3} solution of sodium chloride for 24 h to convert any other ions if present into Na^+ ions. The sodium exchanged zeolite was made chloride free by washing with distilled water and then dried at 100 ºC. The sodium ions were now replaced with bivalent transition metal ions, Co^{2+}, Ni^{2+} or Cu^{2+} by stirring with 0.01 mol dm^{-3} solution of the respective metal chloride for 24 h. It was then filtered and dehydrated at 450 ºC for 4 h [29,30].

Synthesis of *N,N′-bis*(3-hydroxyquinoxaline-2-carboxalidene)ethylenediamine-(QED) (L1): To a solution of 3-hydroxyquinoxaline-2-carboxaldehyde (5 g in 1 L of H_2O) about 2 to 3 drops of conc. HCl was added. An alcoholic solution of ethylenediamine (2 mL in 20 mL alcohol) was added drop by drop until the precipitation was complete. A yellow precipitate was filtered washed with methanol and dried in vacuum over anhydrous calcium chloride (**Scheme-I**).

Synthesis of *N,N′-bis*(3-hydroxyquinoxaline-2-carboxalidene)*o*-phenylenediamine (QPD) (L2): To a 3-hydroxyquinoxaline-2-carboxaldehyde solution (5 g in 1 L H_2O) 2-3 drops of conc. HCl was added with constant stirring and to this solution of *o*-phenylenediamine (2 g in 20 mL H_2O) was added drop by drop. A orange yellow solid obtained was filtered washed and dried over anhydrous calcium chloride (**Scheme-I**).

Preparation of zeolite Y encapsulated complexes: The encapsulation of metal complexes in zeolite Y was achieved by flexible ligand method [31,32]. A general procedure was adopted for the synthesis of the complexes. Metal exchanged zeolite Y (~5 g) was mixed with the ligand dissolved in 50 mL ethanol (1:1 metal: ligand mole ratio) and refluxed on a water bath for about 8 h. The metal complexes thus formed were then Soxhlet extracted with ethanol and dichloromethane for several days until the extract was colourless. This process removes any surface complexes formed on the zeolite. Uncomplexed metal ions present in the zeolite were removed by back exchanging with (0.1 mol dm^{-3}) NaCl solution for 24 h. The zeolite containing the metal complexes was then made chloride free by washing with distilled water and dried in vacuum. The resulting zeolite encapsulated metal complexes are denoted as YMQED and YMQPD where M = Co^{2+}, Ni^{2+} or Cu^{2+} and Y stands for zeolite.

Procedure for catalytic reaction: Hydroxylation of phenol was conducted in a 100 mL batch reactor fitted with a magnetic

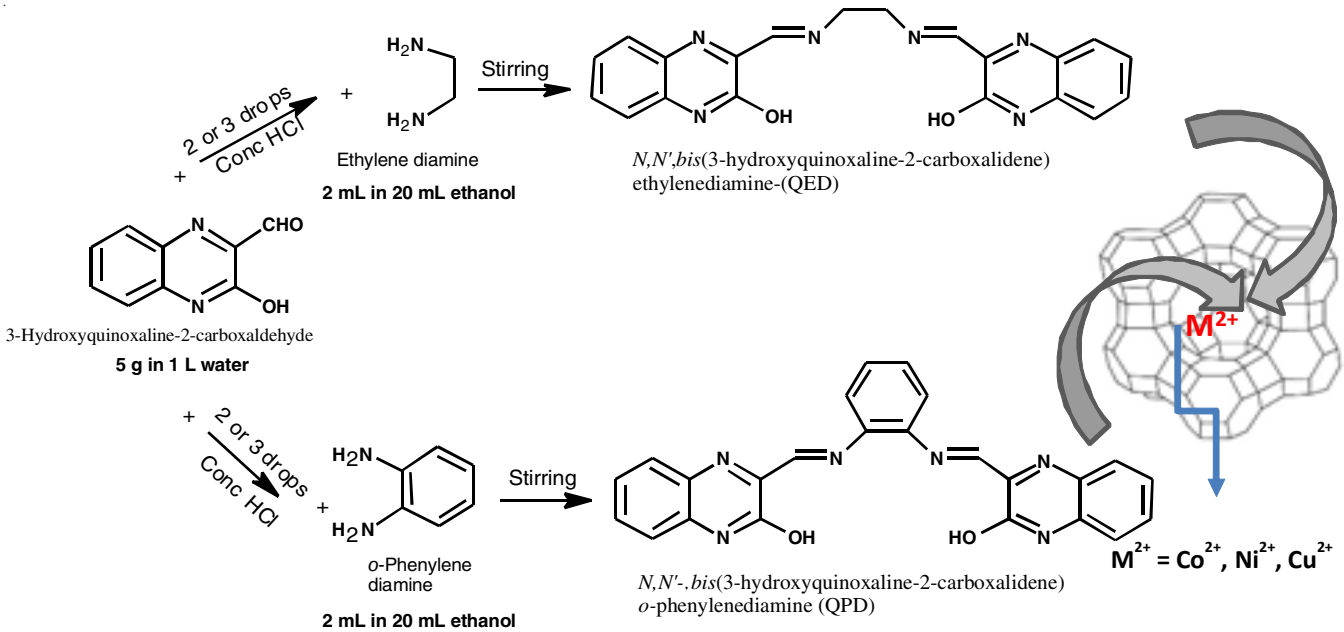

Scheme-I

stirrer. For the general reaction, phenol (2 mL), H_2O_2 (5 mL) and H_2O (5 mL) were taken in a 100 mL round bottom flask and the catalyst (about 0.1 g) was added. The reaction mixture was stirred for 4 h. The reactions were done at three different temperatures. For reactions at higher temperature, oil bath was used. The products of oxidation were analyzed using a Chemito 8510 gas chromatograph equipped with FID detector using a SE-30 column. A blank run was also carried out in the absence of any catalyst, there was no appreciable conversion even after 4 h.

RESULTS AND DISCUSSION

The synthesized metal complexes were analyzed for their elemental composition. The % of silica was estimated by digestion using conc. H_2SO_4. Zeolite encapsulated metal complexes was accurately weighed ('x' g) and transferred to a beaker. Conc. H_2SO_4 (about 40 mL) was added and heated until it just fumes. It was diluted with 200 mL water after cooling and filtered through an ash less filter paper. The residue was dried at 1000 ºC in a platinum crucible, cooled and weighed ('a' g). Then hydrofluoric acid (10 mL) was added when all the silica was removed as SiF_4 and the remaining solid finally ignited to 1000 ºC ('b' g) following the procedure by Abraham [33]. From this the percentage of silica (SiO_2) was calculated using the following equation:

$$SiO_2\ (\%) = \frac{(a-b)}{x} \times 00$$

The residue in the platinum crucible was then fused with potassium persulphate until a clear melt was obtained and dissolved in water, again filtered and combined with earlier filtrate. The Na, Al and transition metal ions in the solution were determined by ICP-AES. From the metal percentages obtained, the ion exchange capacity was calculated and derived the unit cell formula. The CHN analysis was done to obtain the percentage of carbon and nitrogen. The results are given in Table-1.

Surface area and pore volume: Surface area analyses provide a strong evidence for encapsulation according to Mori *et al.* [34] and Satterfield [35]. A decrease in surface area on encapsulation of metal complexes indicates that the pores of the zeolite are filled by metal complexes. This is also supported by a decrease in pore volume. In the case of zeolites, the surface area is largely internal. Hence the inclusion of guest molecules should reduce their absorption capacity. The BET surface area of the metal exchanged zeolite-Y as well as the encapsulated complexes is given in Table-2. It can be seen that surface area of the zeolite encapsulated metal complex is considerably lower than the corresponding metal exchanged zeolite.

TABLE-1a
ELEMENTAL ANALYSIS (%) DATA FOR NaY, YCo AND ZEOLITE ENCAPSULATED COBALT COMPLEXES

Compound	Si	Al	Na	Co	C	N
NaY	19.70	7.90	6.69	–	–	–
YCo	19.72	7.80	4.70	6.02	–	–
YCoQED	19.60	7.71	5.30	4.10	2.14	0.79
YCoQPD	19.71	7.60	5.15	3.75	2.19	0.64

TABLE-1b
ELEMENTAL ANALYSIS (%) DATA FOR YNi AND ZEOLITE ENCAPSULATED NICKEL COMPLEXES

Compound	Si	Al	Na	Ni	C	N
YNi	19.73	7.20	4.28	3.35	–	–
YNiQED	19.60	7.50	6.4	2.58	0.35	0.12
YNiQPD	19.30	7.43	4.48	2.01	1.39	0.41

TABLE-1c
ELEMENTAL ANALYSIS (%) DATA FOR YCu AND ZEOLITE ENCAPSULATED COPPER COMPLEXES

Compound	Si	Al	Na	Cu	C	N
YCu	19.45	7.85	5.81	4.13		
YCuQED	19.30	7.70	5.13	1.18	1.46	0.48
YCuQPD	19.50	7.90	5.75	2.63	4.04	1.26

TABLE-2
SURFACE AREA AND PORE VOLUME DATA OF THE METAL EXCHANGED AND ENCAPSULATED COMPLEXES

	Surface area (Sqm/g)			Pore volume (cc/g)		
	Co	Cu	Ni	Co	Cu	Ni
Y	450	380	420	0.2604	0.2198	0.2494
QED	201	246	277	0.1157	0.1375	0.1621
QPD	330	300	320	0.1818	0.1736	0.1796

X-ray diffraction studies: The XRD provides valuable information on crystallinity as well as any change in unit cell parameters that might arise due to the encapsulation [36,37]. The XRD pattern obtained for all the complexes were similar in nature. As a specimen, XRD patterns of the zeolite encapsulated copper complexes and those of the copper Y zeolite are given in Fig. 1. The patterns revealed that there is no change in the overall crystallinity of the zeolite Y host lattice on encapsulation. Thus, the zeolite framework remains intact during encapsulation.

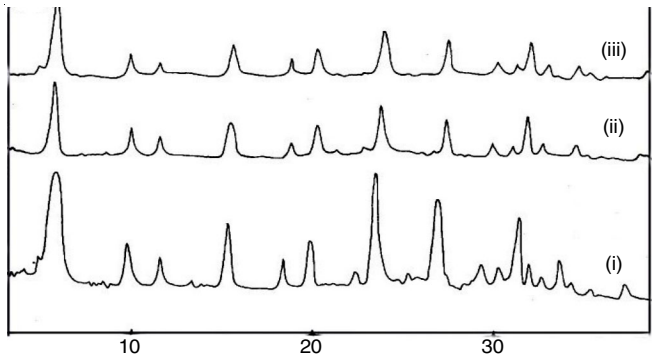

Fig. 1. XRD pattern of (i) CuY (ii) CuYQED (iii) CuY QPD

Scanning electron microscopy studies: Purification of the encapsulated complexes was done by Soxhlet extraction using ethanol and dichloromethane. Studies using SEM of the zeolite encapsulated complexes [32] taken before and after Soxhlet extraction revealed that the extraction process removes all the transition metal complexes formed on the surface. The SEM of zeolite encapsulated cobalt complexes before and after Soxhlet extraction at various magnifications are (as specimen) given in Fig. 2a-b.

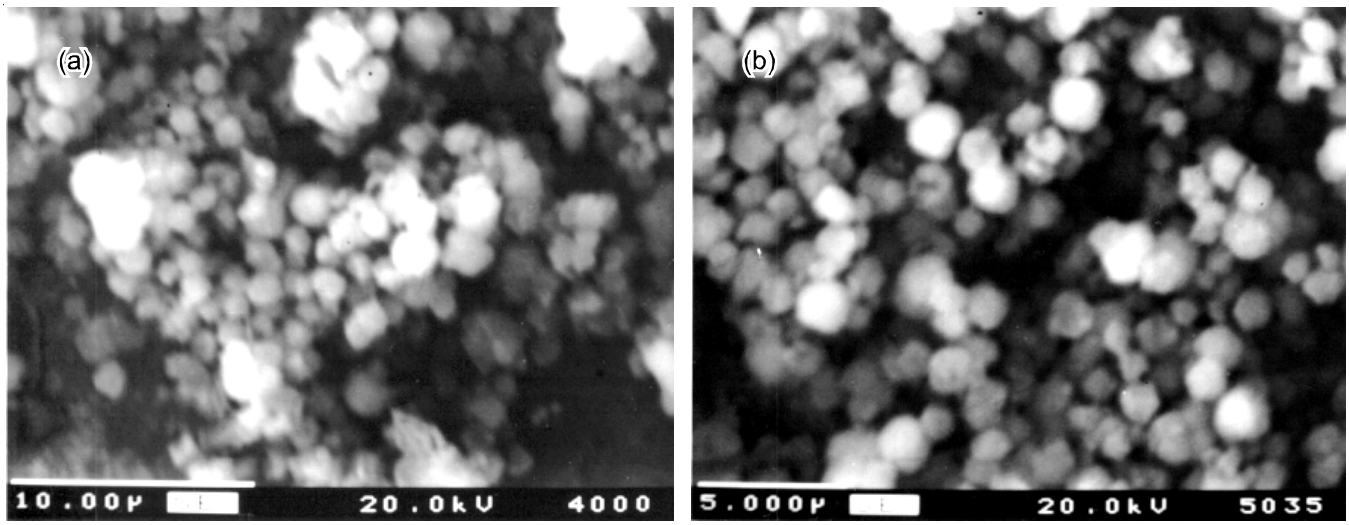

Fig. 2. Scanning electron images (a) before (b) after Soxhlet extraction

Infrared studies: The FTIR data of zeolite encapsulated QED, QPD, complexes are given in Table-3. Bands due to the O-H vibrations of the zeolites lie in the range from 3600-3300 cm^{-1}. Other major zeolite framework bands appear around 1140, 1040, 960, 785 and 740 cm^{-1}. Most of the bands due to ligands are masked by the zeolite peaks. However, the bands due to C=N and enolic C-O could be observed [38-40].

TABLE-3
FTIR SPECTRAL DATA OF THE LIGAND, METAL EXCHANGED ZEOLITE AND ENCAPSULATED COMPLEXES

Compound	N-H	C=N	C-O	Zeolitic peaks	Zeolitic peaks
YCu	–	–	–	1009	569
QED	3568	1659	1564	–	–
YCoQED	3588	1653	1529	999	567
YNiQED	3568	1641	1529	1009	565
YCuQED	3455	1653	1530	1007	569
QPD	3500	1670	1535	–	–
YCoQPD	3436	1649	1527	995	564
YNiQPD	3414	1642	1526	1005	573
YCuQPD	3431	1634	1530	1010	572

The red shift in the azomethine C=N clearly indicates that the ligand is coordinated to the metal atom through this nitrogen. The C-O (phenolic) stretching which appears at 1230 cm^{-1} could not be seen. Probably it might have been obscured by the broad asymmetric stretching mode of the internal tetrahedra in the zeolite framework. Schiff base ligands obtained from 3-hydroxyquinoxaline-2-carboxaldehyde exists in keto-enol tautomerism. In present case, this is indicated by the presence of enolic C-O stretching band (in the spectra of ligand), which shifts to lower frequency on complexation. Such a shift was observed in the present case. Thus in all the complexes, the coordination of the ligands is through the azomethine nitrogen as well as through the oxygen of hydroxyl group.

EPR studies: The EPR technique enables us to determine the electronic state and the symmetry of the ligand field in metal exchanged zeolites. Several studies on the EPR of the zeolite encapsulated cobalt and copper complexes have been carried out [41,42]. The EPR spectra of the present complexes were obtained at liquid nitrogen temperature.

The EPR of Co^{2+} is very sensitive to coordination. The bands obtained for zeolite encapsulated YCoQED and YCoQPD complexes were very broad. Usually spin transition or thermal vibrations decrease the life time of the excited state and due to this EPR spectrum becomes broad. But square pyramidal as well as square planar cobalt complexes are known to exhibit good EPR spectra. The EPR spectra obtained for the nickel(II) complexes, YNiQED and YNiQPD did not provide any valuable information. EPR parameters of the copper complexes are given in Table-4. The $g_\perp$ and $g_\parallel$ values of all the complexes were determined. The in plane covalence parameter α^2 and bonding parameter P are determined from the EPR spectra. The EPR spectra of complexes of QED are shown in Fig. 3.

TABLE-4
EPR PARAMETER OF THE COPPER Y AND ENCAPSULATED COPPER COMPLEXES

Compound	$g_\perp$	$A_\perp$	$g_\parallel$	$A_\parallel$	α^2	P	$g_\parallel/A_\parallel$
Ycu	2.08	66	2.37	136	0.75	-0.88	173
YCuQED	2.05	113	2.22	170	0.85	-0.85	130
YCuQPD	2.07	120	2.34	160	0.94	-0.87	146

All the metal complexes have $g_\parallel > g_\perp$, indicating an axial geo-metry. Copper(II) complexes are unlikely of having a regular octahedral geometry due to Jahn-Teller distortions. Sakaguchi *et al.* [43] reported that the quotient $g_\parallel/A_\parallel$ is an indication of extend of tetragonal distortion. The quotient ranges from 105 to 135 cm for square planar structures. A value of 130 cm obtained for YCuQED, therefore support a square planar structure for the complex.

Magnetic moment: In present study, magnetic susceptibility measurements were done using a Guoy balance and the values were obtained after applying necessary diamagnetic correction. Reports on the magnetic study of zeolite encapsulated metal complexes are few because most of the complexes behave as diamagnetic due to the large zeolite framework. The results obtained from the magnetic moment measurements are shown

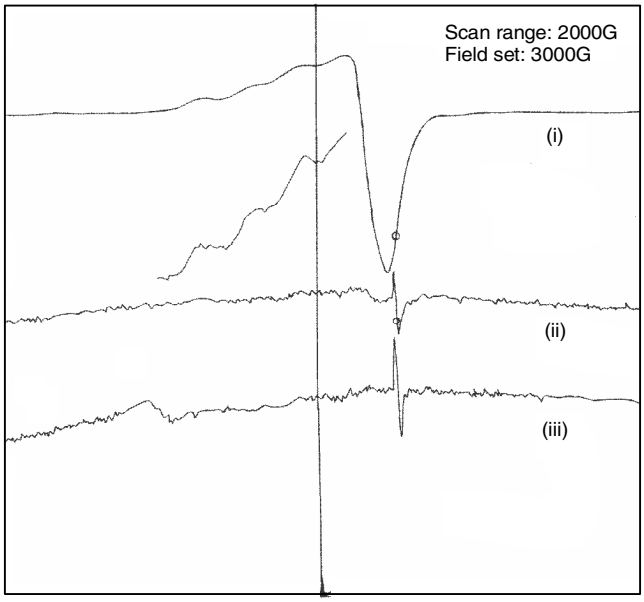

Fig. 3. EPR spectra of the complexes of QED

in Table-5 and some useful inferences were drawn from this study. These inferences can be taken only as a qualitative guide in suggesting the structure.

TABLE-5
MAGNETIC MOMENT DATA OF THE ZEOLITE ENCAPSULATED AND NEAT COMPLEXES

Complexes	Magnetic moment of zeolite-Y encapsulated complexes (BM)	Magnetic moment of neat complexes (BM)
CoQED	5.0	3.97
CoQPD	4.9	3.89
NiQED	4.3	2.30
NiQPD	3.1	2.10
CuQED	2.00	1.95
CuQPD	1.75	1.70

Magnetic susceptibility measurement as a function of dehydration has been studied for the cobalt exchanged zeolite Y. Such systems are attractive choice for magnetic study because of the large difference in magnetic susceptibility shown by cobalt ions in different coordination. The earlier studies have indicated that in case of fully hydrated YCo, magnetic moment (μ_{eff}) suggests an octahedral coordination. Cobalt ions in the supercages (α-cages) have different coordination to that in sodalite (β-cage). Both four and six coordinate cobalt may be present in the cage. Paramagnetic susceptibility of Co^{2+} in zeolite Y often becomes complicated due to a small field dependence arising from ferromagnetic impurities (0.18 atoms of Fe per unit cell). Therefore the magnetic susceptibility of NaY was measured and this value was used for diamagnetic correction. The magnetic moment values of the zeolite encapsulated complexes are given in Table-5. The magnetic moment values of the neat complexes are also included in this table for the sake of comparison.

The neat complex of cobalt with ligand QED is a dimer with the formula $[Co(QED)]_2$. This complex has a magnetic moment of 3.97 B.M. The zeolite encapsulated complex of the same ligand has a μ_{eff} value of 5.0 B.M., which suggest an octahedral geometry for the complex. The YCoQPD also may have an octahedral geometry as its magnetic moment value is 4.9 B.M. Thus, there is a change in the structure of complexes on encapsulation.

The spin only magnetic moment for nickel(II) is 2.83 B.M. For tetrahedral nickel complexes the magnetic moment values lie between 3.2-4.1 B.M. and for octahedral complexes the magnetic moment value is between 2.9-3.3 B.M. YNiQED has a magnetic moment value of 4.3 B.M. indicating a tetrahedral coordination and magnetic moment value of 3.1 B.M. for YNiQPD hints towards an octahedral structure for this complex. The simple complexes $[Ni(QED)]_2$ is a dimers and NiQPD is a monomer. All these complexes exhibit somewhat lower magnetic moment value than the spin only value of 2.83 B.M. This has been attributed to reduced singlet-triplet transition in the case of simple complexes. The values are higher in the case of the encapsulated complexes and the results suggest change in the structure of all the nickel complexes on encapsulation.

Magnetic moment values of the copper complexes lies in the range of 1.75-2.20 B.M. regardless of the stereochemistry. YCuQED has a magnetic moment of 2.0 B.M., which is due to higher spin orbit couplin. These values suggested a distorted square planar structure. Magnetic moment value of 1.95 B.M. is reported for the simple complex $Cu(QED)_2$. The magnetic moment data for the complexes are given in Table-5.

Zeolite encapsulated YCuQPD complexes exhibit magnetic moment values of 1.75 B.M and suggests an octahedral structure for these complexes. The lower magnetic moment of the neat complex is reported to be due to the antiferromagnetic coupling of copper atom. Such a coupling is absent in the encapsulated complex.

Electronic spectra: The electronic spectra of all the zeolite encapsulated metal complexes were measured in the diffuse reflectance mode because of the insolubility of the zeolite encapsulated complexes. The location and coordination taken up by the charge balancing cations and the complexes in the zeolite could be obtained from the electronic spectra of the complexes as reported by Maurya *et al.* [44]. The spectra combined with the EPR data and magnetic measurements can be used to predict the probable structure of the zeolite encapsulated metal complexes. The UV-visible diffuse reflectance spectra of the zeolite encapsulated as well as the simple complexes are given in Fig. 4a-b.

YCoQED shows absorptions at 29820, 23920, 17830 and 15480 cm^{-1}. These values suggest a six coordinated octahedral coordination. Moreover, the complex is EPR silent indicating an octahedral structure with the ligand in a planar symmetry and the other coordination sites occupied by zeolite oxygen or water molecules. The YCoQPD complex also exhibits transitions characteristic of octahedral complexes. The absorptions are obtained at 28520, 23400, 17670 and 13500 cm^{-1}. The YNiQED complexes exhibit bands characteristic of tetrahedral complexes. The complex has bands at 14390 and 13400 cm^{-1}. Goodgame *et al.* [45] studied the tetrahedral complex, $NiBr_4^{2-}$, which also has bands at 13230, 14140 cm^{-1}. Therefore YNiQED may also have a tetrahedral structure. The absorption maxima

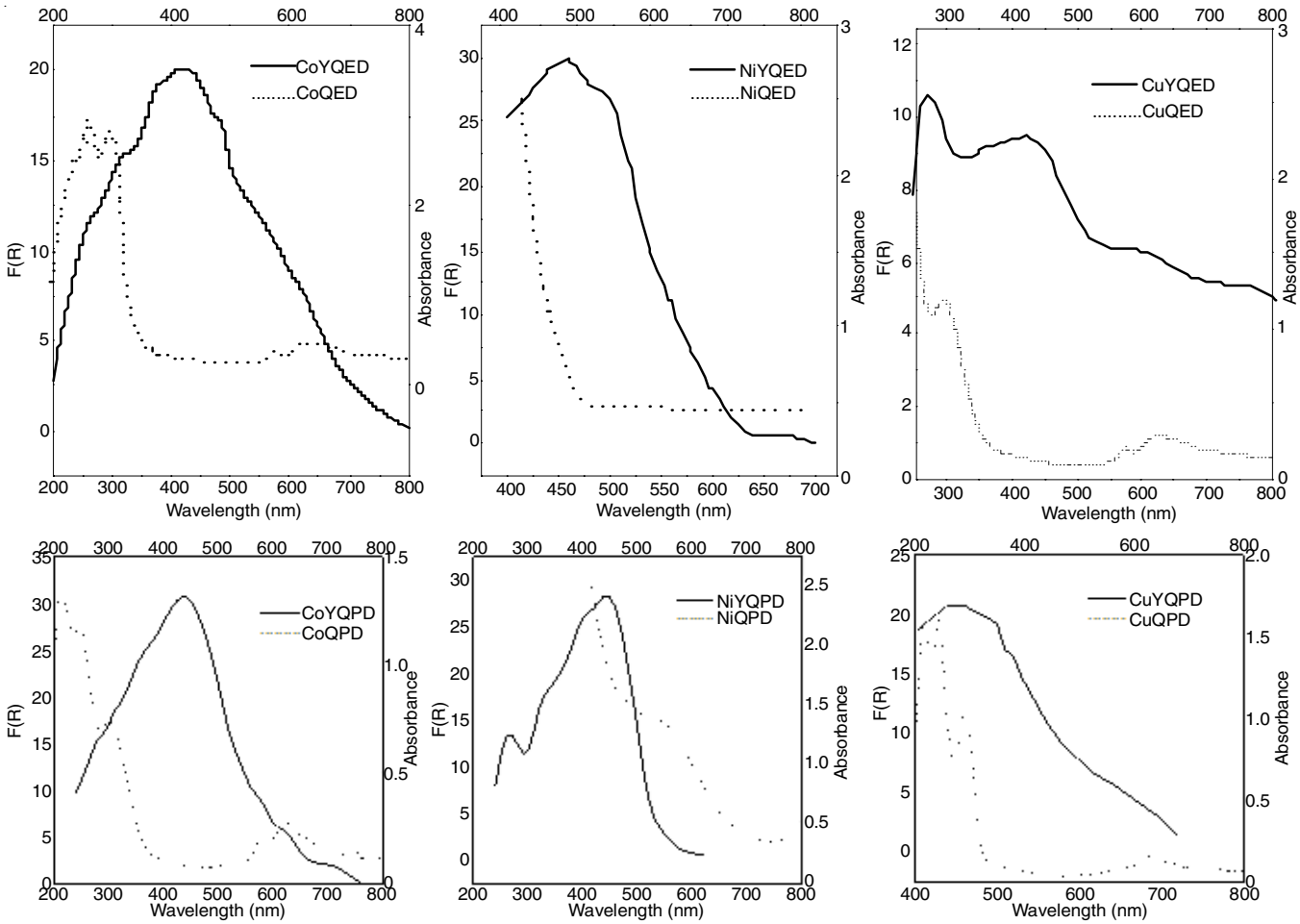

Fig. 4. Diffuse reflectance spectra of QED and QPD complexes

in the case YNiQPD were observed at 35000, 28230, 23000, 21500, 16500 cm^{-1} and these values suggest an octahedral coordination. This compound did not give EPR spectra. Therefore, the complex may exist as a square planar complex at LNT. This can be expected as ligand QPD has a rigid structure.

The YCuQED complex exhibits transitions at 31100, 23300, 16700 and14980 cm^{-1}, indicating a pseudo-tetrahedral structure. Tetrahedral copper(II) complexes are invariably distorted. Four coordinate square planar structure is strongly favoured for a d^9 electronic configuration. The distortion from the tetrahedra involves flattening to square planar geometry. YCuQPD, may be assigned a tetragonally distorted octahedral geometry. A regular octahedral geometry is rare in the case of copper complexes due to Jahn-Teller distortions. For a regular octahedral geometry only one transition should be observed $^2E \leftarrow {}^2T$.

TG analysis: According to Hatakeyama & Liu [46] thermal analysis is a useful tool to study the decomposition pattern of metal complexes encapsulated in zeolite Y cages. The TG/DTG plots of the complexes are given in Fig. 5. A weight loss of about 15-16% is observed in the temperature range 30-300 ºC (Table-6). Such a weight loss is observed in the case of the metal exchanged zeolite also. Therefore, this may be due to the loss of intrazeolite water molecules. IR spectra of the complexes obtained after heating to 300 ºC is found to be exactly similar to that of the original complex indicating that there is no decomposition of the complex taking place in this range. Further decomposition of the complexes takes place in a single step. However, small weight loss is observed later in certain cases. In case of YNiQPD, the loss of intrazeolite water and ligands could not be distinguished as they occur in the same range. The variation in the thermal decomposition pattern exhibited by different complexes is an indication of formation of metal complexes. The amount of intrazeolite metal complex can be roughly calculated from the weight loss. It is seen from Table-6 that about 5% weight loss occurs during the second stage of decomposition. Probably this weight loss might be due to the decomposition of the complex within the zeolite. Therefore for comparing the stabilities of the complexes, the peak temperature in the second stage of decomposition was considered. For all the complexes, there was about 20-25% weight loss in the temperature range from 50-600 ºC. Zeolite framework is seen to be decomposed only above 793 ºC. Among the copper complexes, the order of stability was as follows: YCuQPD > YCuQED. The order of stability of cobalt, nickel and copper complexes is as follows:

YNiQED > YCuQED > YCoQED

YCoQPD > YCuQPD > YNiQPD

Catalytic activity studies: Initial screening studies showed that among the various metal-complexes, copper complexes

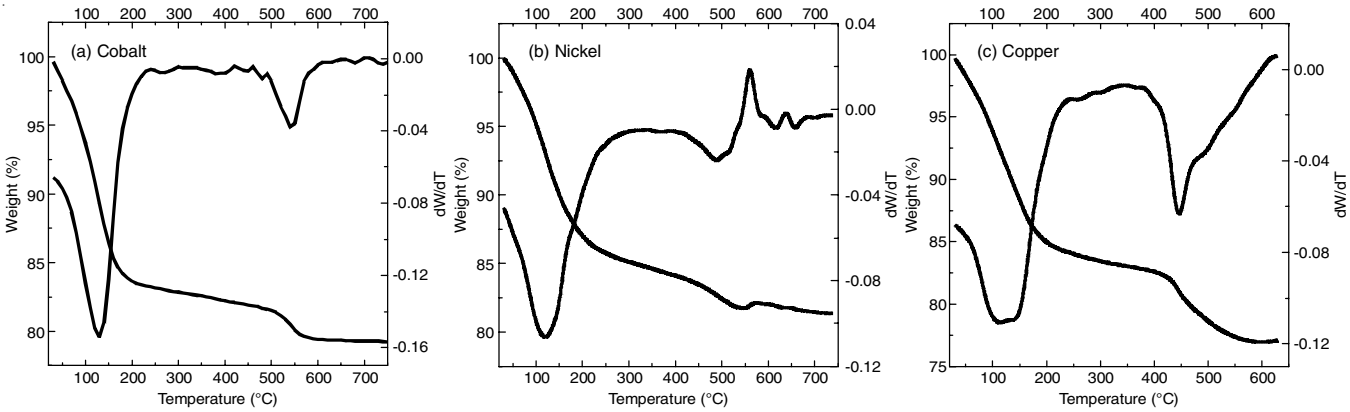

Fig. 5. TG/DTG curves zeolite encapsulated QED complexes

TABLE-6
TG/DTG DATA OF THE ENCAPSULATED COMPLEXES

Compound	Weight loss: Stage I			Weight loss: Stage II		
	Temp. range (°C)	Peak temp. (°C)	Mass loss (%)	Temp. range (°C)	Peak temp. (°C)	Mass loss (%)
YCoQED	50-250	127	15	310-600	298	4.5
YNiQED	50-300	143	16	350-500	606	3.0
YCuQED	50-250	116	14	300-650	450	7.0
YCoQPD	50-350	117	16	355-600	552	4.1
YNiQPD	50-320	161	16	–	–	–
YCuQPD	50-350	104	16	350-500	4610	4.6

show the maximum catalytic activity. A study of hydroxylation of phenol using both the neat as well as zeolite encapsulated copper complexes of various ligands was carried out. The results of variation of phenol/H_2O_2 ratio are given in Table-7. It can be seen that in the case of zeolite encapsulated complexes the conversion % increases with increase in H_2O_2/phenol ratio. It was also seen that the conversion into the industrially more useful hydroquinone was increasing with increase in H_2O_2/phenol ratio. An interesting fact observed was that in case of CuYOPD complex, there is a preference or selectivity towards catechol. The catechol to hydroquinone ratio, which followed a statistical ratio of 2:1 in the case of homogeneous complexes, due to the availability of two *ortho*-positions, approached a ratio close to 1 in the case of zeolite encapsulated complexes (Fig. 6). This may be due to the shape selectivity of the zeolite pore. In the case of neat complexes, the conversion showed a sharp increase when the H_2O_2/phenol ratio was increased from 1 to 2.5 (Table-7). But when H_2O_2/phenol ratio increased from 2.5 to 5, even though the conversion % was increased the selectivity towards hydroquinone showed a decrease. This may be due to the conversion of phenol into unwanted tarry products. Inspite of the higher metal percentage of the neat complexes, the conversion percent is higher for zeolite encapsulated complex. When the turn over number (TON) was calculated for the neat complex as well as the zeolite metal encapsulated complexes (Table-8), it was found the TON was ten times more for the zeolite encapsulated metal complexes. The order of reactivity of zeolite encapsulated complexes containing various ligands may be given as CuYQED > CuYQPD. For neat complexes, the order of reactivity was similar CuQED > CuQPD. The proposed mechanism for the reaction is shown in Fig. 6.

Conclusion

Zeolite encapsulated cobalt(II), nickel(II) and copper(II) complexes of Schiff bases derived from 3-hydroxyquinoxaline-2-carboxaldehyde has been successfully encapsulated in the zeolite Y. The unit cell formulae of the complexes were determined from the elemental analysis. The XRD and SEM studies indicated that there is no surface complexes remaining and the zeolite framework was retained as such without dealumi-

TABLE-7
EFFECT OF PHENOL/H_2O_2 RATIO ON PERCENTAGE CONVERSION OF PHENOL IN THE CASE OF ZEOLITE ENCAPSULATED COMPLEXES AS WELL AS NEAT COMPLEXES

Catalyst	Volume ratio (phenol:H_2O_2)								
	1:1			1:2.5			1:5		
	%Con	CAT	HQ	%Con	CAT	HQ	%Con	CAT	HQ
CuYQED	18	54.0	46.0	36.5	50	50	61	41	58.9
CuYQPD	21	53.3	46.6	48.7	52	48	57	45.2	54.8
CuQED	2.0	39.7	34.7	28.0	63	37	44	89.5	10.5
CuQPD	2.5	99.0	1.0	34.0	66	34	37	99.0	1.0

Temp: 30 °C, Catalyst amount: 0.1 g, Time: 4 h, Solvent: water

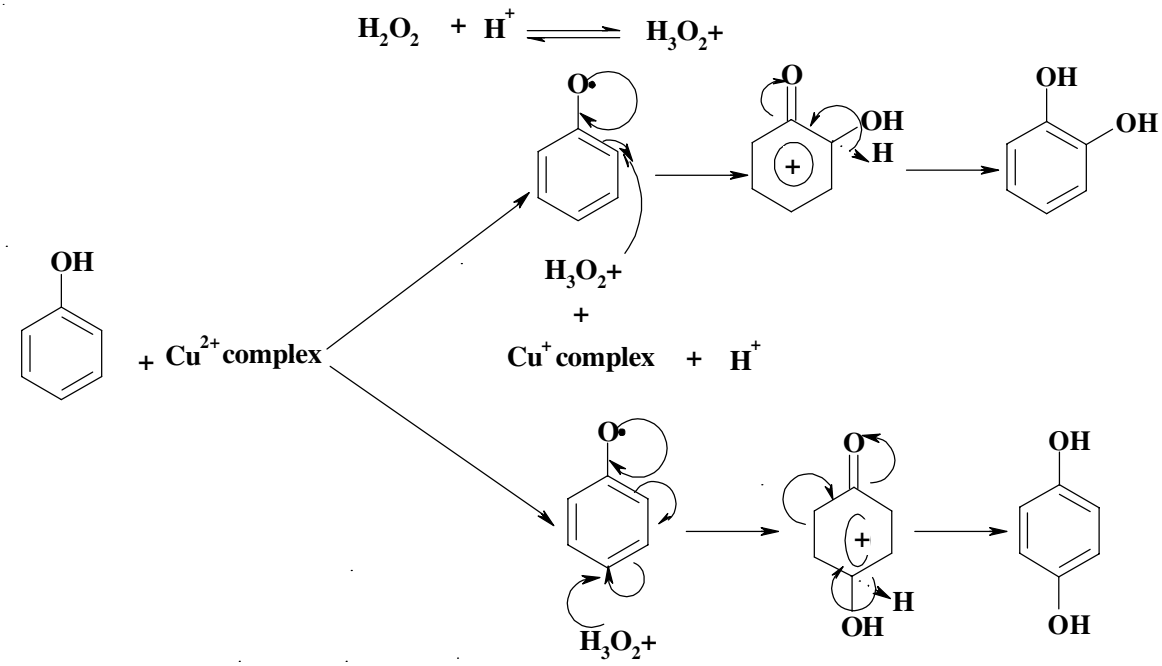

Fig. 6. Mechanism of hydroxylation of phenol

TABLE-8
TON OF THE ZEOLITE ENCAPSULATED AS WELL AS NEAT COMPLEXES OF COPPER (PHENOL:H_2O_2 RATIO 1:2.5) CATALYST: 0.1 g

	% Metal × 10^3		TON (Conversion % per g of metal per h) × 10^{-3}	
	Encapsulated complexes	Neat complexes	Encapsulated complexes	Neat complexes
QED	1.17	14.47	7.76	0.483
QPD	2.63	13.36	4.62	0.636

nation. The surface area and pore volumes decreased indicating the encapsulation of metal complexes inside the pores. Among the cobalt complexes, the electronic and magnetic moment values suggested an octahedral structure for YCoQED and YCoQPD. The NiYQED was assigned as a tetrahedral geometry. NiYOPD complex was EPR silent hinting the possibility of square planar-octahedral equilibrium in this case, which was evident from the magnetic moment, spectral as well as EPR spectral values. The CuYQED complex was assigned a pseudo-tetrahedral structure based on the electronic spectra, EPR and magnetic moment value of 2.0 B.M. The thermal analysis could give an inference about the relative stability of the different complexes. The copper complexes were found to be efficient catalyst for phenol hydroxylation and their activity indicated that they were more efficient than homogenous catalyst.

ACKNOWLEDGEMENTS

The authors thank Department of Applied Chemistry, Cochin University of Science and Technology, RSIC Chennai and CDRI Lucknow, India for providing the spectral facilities.

CONFLICT OF INTEREST

The authors declare that there is no conflict of interests regarding the publication of this article.

REFERENCES

1. R.A Sheldon, *Green Chem*., **7**, 267 (2005); https://doi.org/10.1039/B418069K
2. M.E. Ali, M.M. Rahman, S.M. Sarkar and S.B.A. Hamid, *J. Nanometer*., **2014**, 192038 (2014); https://doi.org/10.1155/2014/192038
3. B. Dutta, S. Jana, R. Bera, P.K. Saha and S. Koner, *Appl. Catal. A*, **318**, 89 (2007); https://doi.org/10.1016/j.apcata.2006.10.041
4. A.H. Ahmed, *Rev. Inorg. Chem.*, **34**, 153 (2014); https://doi.org/10.1515/revic-2013-0013
5. D.R. Godhani, H.D. Nakum, D.K. Parmar, J.P. Mehta and N.C. Desai, *Inorg. Chem. Commun.*, **72**, 105 (2016); https://doi.org/10.1016/j.inoche.2016.08.017
6. N. Kosinov, C. Liu, E.J.M. Hensen and E.A. Pidko, *Chem. Mater.*, **30**, 3177 (2018); https://doi.org/10.1021/acs.chemmater.8b01311
7. C.K. Modi, P.M. Trivedi, J.A. Chudasama, H.D. Nakum, D.K. Parmar, S.K. Gupta and P.K. Jha, *Green Chem. Lett. Rev.*, **7**, 278 (2014); https://doi.org/10.1080/17518253.2014.946101
8. Y. Li, L. Li and J. Yu, *Chem*, **3**, 928 (2017); https://doi.org/10.1016/j.chempr.2017.10.009
9. D. Xu, H. Lv and B. Liu, *Front. Chem.*, **6**, 550 (2018); https://doi.org/10.3389/fchem.2018.00550
10. I.Kuzniarska-Biernacka, K. Biernacki, A.L. Magalhães, A.M. Fonseca, and I.C. Neves, *J. Catal.*, **278**, 102 (2011); https://doi.org/10.1016/j.jcat.2010.11.022
11. A. Corma and H. Garcia, *Eur. J. Inorg. Chem.*, 1143 (2004); https://doi.org/10.1002/ejic.200300831
12. J.M. Thomas and R. Raja, *Stud. Surf. Sci. Catal.*, **148**, 163 (2004); https://doi.org/10.1016/S0167-2991(04)80198-8
13. B. Meier, T. Werner, I. Klimant and O.S. Wolfbeis, *Sens. Actuators B Chem.*, **29**, 240 (1995); https://doi.org/10.1016/0925-4005(95)01689-9
14. M.M. Heravi, B. Heidari, V. Zadsirjan and L. Mohammadi, *RSC Adv*., **10**, 24893 (2020); https://doi.org/10.1039/D0RA02341H
15. F. Bedioui, *Coord. Chem. Rev.*, **144**, 39 (1995); https://doi.org/10.1016/0010-8545(94)08000-H
16. K.J. Balkus Jr. and A.G. Gabrielov, *J. Incl. Phenom. Macrocycl. Chem.*, **21**, 159 (1995); https://doi.org/10.1007/BF00709415

17. C. Dai, K. Du, C. Song and X. Guo, *Adv. Catal.*, **67**, 91 (2020); https://doi.org/10.1016/bs.acat.2020.10.001
18. Z. Khodadadi and R. Mahmoudian, *React. Kinet. Mech. Catal.*, **119**, 685 (2016); https://doi.org/10.1007/s11144-016-1072-z
19. R.J. Taylor, R.S. Drago and J.E. George, *J. Am. Chem. Soc.*, **111**, 6610 (1989); https://doi.org/10.1021/ja00199a020
20. S. Deshpande, D. Srinivas and P. Ratnasamy, *J. Catal.*, **188**, 261 (1999); https://doi.org/10.1006/jcat.1999.2662
21. K.K. Bania and R.C. Deka, *J. Phys. Chem. C*, **115**, 9601 (2011); https://doi.org/10.1021/jp2003672
22. H.B. Li, C. Qin, W.B. Yang, X.P. Hu and S.Y. Qin, *Chin. Chem. Lett.*, **18**, 103 (2007); https://doi.org/10.1016/j.cclet.2006.11.011
23. A.A.A. Emara, A.M. Ali, A.F. El-Asmy and E.-S.M. Ragab, *J. Saudi Chem. Soc.*, **18**, 762 (2014); https://doi.org/10.1016/j.jscs.2011.08.002
24. N. Herron, *Inorg. Chem.*, **25**, 4714 (1986); https://doi.org/10.1021/ic00246a025
25. F. Bedioui, L. Roue, J. Devynck and K.J. Balkus Jr., *Stud. Surf. Sci. Catal.*, **84**, 917 (1994); https://doi.org/10.1016/S0167-2991(08)63624-1
26. K.J. Balkus Jr., A.A. Welch and B.E. Gnade, *Zeolites*, **10**, 722 (1990); https://doi.org/10.1016/0144-2449(90)90053-T
27. C.J. Dhanaraj, J. Johnson, J. Joseph and R.S. Joseyphus, *J. Coord. Chem.*, **66**, 1416 (2013); https://doi.org/10.1080/00958972.2013.782008
28. J. Mathew, Ph.D. Thesis, Cochin University of Science and Technology, Cochin, India (1995).
29. C. Naccache and B.T.Z. Younès, Science and Technology, Springer (1984).
30. L. Wu and A. Navrotsky, *Phys. Chem. Chem. Phys.*, **18**, 10116 (2016); https://doi.org/10.1039/C5CP07918G
31. C.R Jacob., S.P. Varkey and P. Ratnasamy, *Appl. Catal. A*, **168**, 353 (1998); https://doi.org/10.1016/S0926-860X(97)00365-7
32. J. Poltowicz, K. Pamin, E. Tabor, J. Haber, A. Adamski and Z. Sojka, *Appl. Catal. A*, **299**, 235 (2006); https://doi.org/10.1016/j.apcata.2005.10.034.
33. R. Abraham, Ph.D. Thesis, Cochin University of Science and Technology, Cochin, India (1999).
34. K. Mori, K. Kagohara and H. Yamashita, *J. Phys. Chem. C*, **112**, 2593 (2008); https://doi.org/10.1021/jp709571v
35. C.N. Satterfield, Heterogeneous Catalysis in Industrial Practice, McGraw-Hill, Singapore Ed. 2 (1993).
36. P. Gallezot, Y. Ben Taarit and B. Imelik, *J. Catal.*, **26**, 295 (1972); https://doi.org/10.1016/0021-9517(72)90087-5
37. D. Simpson and H. Steinfink, *J. Am. Chem. Soc.*, **91**, 6225 (1969); https://doi.org/10.1021/ja01051a003
38. S.P. Varkey, C. Ratnasamy and P. Ratnasamy, *J. Mol. Catal. Chem.*, **135**, 295 (1998); https://doi.org/10.1016/S1381-1169(97)00307-5
39. A.H. Kianfar, L. Keramat, M. Dostani, M. Shamsipur, M. Roushani and F. Nikpour, *Spectrochim. Acta A Mol. Spectrosc.*, **77**, 424 (2010); https://doi.org/10.1016/j.saa.2010.06.008
40. V. Arun, S. Mathew, P.P. Robinson, M. Jose, V.P.N. Nampoori and K.K.M. Yusuff, *Dyes Pigments*, **87**, 149 (2010); https://doi.org/10.1016/j.dyepig.2009.01.010
41. S. Chavan, D. Srinivas, P. Ratnasamy, *J. Catal.*, **192**, 286 (2000); https://doi.org/10.1006/jcat.2000.2851
42. S.P. Varkey and C.R. Jacob, *Indian J. Chem.*, **38A**, 320 (1999).
43. U. Sakaguchi and A.W. Addison, *J. Chem. Soc., Dalton Trans.*, **4**, 600 (1979); https://doi.org/10.1039/dt9790000600
44. M.R. Maurya, A.K. Chandrakar and S. Chand, *J. Mol. Catal. Chem.*, **274**, 192 (2007); https://doi.org/10.1016/j.molcata.2007.05.018
45. M. Goodgame, D.M.L. Goodgame and F.A. Cotton, *J. Am. Chem. Soc.*, **83**, 4161 (1961); https://doi.org/10.1021/ja01481a014
46. T. Hatakeyama and Z. Liu, Handbook of Thermal Analysis, John Wiley and Sons: New York (1998).
47. M.R. Maurya, H. Saklani, A. Kumar and S. Chand, *Catal. Lett.*, **93**, 121 (2004); https://doi.org/10.1023/B:CATL.0000016959.93948.d7
48. K.K. Bania and R.C. Deka, *J. Phys. Chem. C*, **117**, 11663 (2013); https://doi.org/10.1021/jp402439x